Excited Electronic States of carotenoids; Time-Dependent Density-Matrix-Response Algorithm

Sergei Tretiak, Vladimir Chernyak, and Shaul Mukamel[*]

Department of Chemistry and Rochester Theory Center for Optical Science and Engineering, University of Rochester, Rochester, New York 14627

ABSTRACT: The response of the single-electron density matrix of a many-electron system to an external field is calculated using the Time-Dependent Hartree-Fock (TDHF) technique. A procedure for inverting the resulting nonlinear response functions to obtain an effective quantum multilevel system that has the same response is developed. The number of effective states is gradually increased as higher-order nonlinearities are computed. The complete set of intrastate and interstate density matrices and excited state energies can be calculated. A favorable N-scaling of computational effort with size can be obtained making use the localization of the optical transitions in real space. © 1998 John Wiley & Sons, Inc. Int J Quant Chem 70: 711-727, 1998

Key words: Density Matrix Response Functions, N-scaling, Time-Dependent Hartree-Fock, Nonlinear Response, Bosonization, Carotenoids.

I. INTRODUCTION

The complete information on the optical response of a quantum system is contained in its set of many-electron eigenstates $|\nu\rangle, |\eta\rangle, \ldots$ and energies $\epsilon_\nu, \epsilon_\eta, \ldots$ [1]. Since the number of states increases exponentially with the number of electrons, exact calculations become impractical even for fairy small molecules with a few atoms. An approximation at some level of configuration interaction (CI) allows to compute the states, and optical susceptibilities may be calculated using a summation over states (SOS) [2–5]. The CI/SOS is computationally expensive. In addition, size consistency is not guaranteed *a priori* and special care needs to be taken when choosing the right configurations.

Using the many-electron wavefunctions it is possible to calculate all n-body quantities and correlations. Most of this information is, however, rarely used in the calculation of common observables (energies, dipole moments, spectra, *etc.*) which only depend on the

expectation values of one- and two- electron quantities. A reduced description which only keeps a small amount of relevant information is called for. An important example of such a method is density-functional theory (DFT) [6–11] which only retains the ground state charge density profile:

$$\rho_{nn}^{gg} = \langle g|c_n^+ c_n|g\rangle \ , \tag{1.1}$$

where $|g\rangle$ denotes the ground-state many-electron wavefunction and $c_n^+(c_n)$ is the Fermi annihilation (creation) operators for the n-th basis set orbital. Hohenberg and Kohn's theorem proves that the ground state energy is a unique and a universal functional of ρ_{nn} [12,13], making it possible to compute self consistently the charge distribution and the ground state energy. This approach has been remarkably successful, and extensions to excited states have been made as well [10,11].

In this paper we develop a semiclassical approach for calculating the excited state energies ϵ_ν, and density matrices

$$\rho_{nm}^{\nu\eta} \equiv \langle \nu|c_n^+ c_m|\eta\rangle \ . \tag{1.2}$$

This approach is formally unrelated to DFT. Nevertheless, it shares its basic philosophy of aiming at "the truth but not the whole truth". We recall that $|\nu\rangle$ and $|\eta\rangle$ represent the global electronic states of the system, whereas n and m denote the atomic basis functions. These quantities carry more information than ρ_{nn}^{gg}, yet considerably less than the complete set of eigenstates. $\rho^{\nu\nu}$ is the reduced single-electron density matrix of state ν. For $\nu \neq \eta$ $\rho^{\nu\eta}$ is the density-matrix associated with the transition between ν and η. When the system is driven by an optical field, its wavefunction becomes a coherent superposition states

$$\Psi(t) = \sum_\nu a_\nu(t)|\nu\rangle \ , \tag{1.3}$$

and its density matrix is given by

$$\rho_{nm}(t) \equiv \langle \Psi(t)|c_n^+ c_m|\Psi(t)\rangle = \sum_{\nu\eta} a_\nu^*(t)a_\eta(t)\rho_{nm}^{\nu\eta} \ . \tag{1.4}$$

$\rho_{nm}^{\nu\eta}$ are thus the building blocks for the time-dependent single-electron density matrix. In addition, the density matrix provides the complete information necessary for computing the matrix elements of all single-electron operators. Given the operator

$$\mu = \sum_{nm} \mu_{nm} c_n^+ c_n \ , \tag{1.5}$$

we have

$$\langle \nu|\mu|\eta\rangle = \sum_{nm} \mu_{nm}\rho_{nm}^{\nu\eta} \ . \tag{1.6}$$

In particular, dipole matrix elements which determine on the optical properties have the form of Eq. (1.6).

Our approach starts by coupling the molecule to an external field $\mathcal{E}(t)$ through

$$H_{int} = -\mu \mathcal{E}(t) \equiv \sum_{nm} \mathcal{E}_{nm}(t) c_n^+ c_m \ . \tag{1.7}$$

Where $\mathcal{E}_{nm}(t) \equiv \mu_{nm}\mathcal{E}(t)$. We can then expand the induced density matrix in powers of the incoming field

$$\rho_{nm}(t) = \rho_{nm}^{gg} + \int d\tau \sum_{n'm'} S_{nm,n'm'}^{(1)}(t;\tau) \mathcal{E}_{n'm'}(\tau)$$

$$+ \int \int d\tau_1 d\tau_2 \sum_{\substack{n'm' \\ n''m''}} S_{nm,n'm',n''m''}^{(2)}(t;\tau_1,\tau_2) \mathcal{E}_{n'm'}(\tau_1) \mathcal{E}_{n''m''}(\tau_2) + \dots \ . \tag{1.8}$$

The j-th order density-matrix response functions (DMRF) $S^{(j)}$ can be conveniently calculated using the Time-Dependent Hartree-Fock (TDHF) approximation [18–20], which provides a closed system of equations for the reduced single-electron density-matrix ρ_{mn}. Since the DMRF can be alternatively expanded in terms of the system energies and matrix elements of the single-electron operators $c_m^+ c_n$, it constitutes a source of information on these quantities. However, it is not easy to interpret the TDHF response in terms of the global eigenstates since the structure of the TDHF expressions is very different from their standard SOS counterparts.

The present article provides an algorithm for inverting the DMRF to obtain an effective multilevel system which has the same response functions, resulting in the eigenvalues and all density matrix elements (Eq. (1.2)). Note that the DMRF are more general than the optical response functions since the interaction (Eq. (1.7)) is not limited to the dipole operator. The latter has often selection rules which limit the information to a few dominant states. The freedom to use any field $\mathcal{E}_{nm}(t)$ in Eq. (1.7) allows us to calculate all possible states.

The effective multilevel system will be constructed in four steps (Fig. 1).

(i) Starting with the original quantum fermion model QFM we build its classical limit by considering the space of single Slater determinants $\mathbf{M}$ (the space of coherent states as its phase space). The Poisson bracket on $\mathbf{M}$ and the classical Hamiltonian have been introduced in [21]. We make use of the observation [22] that the TDHF approximation can be considered as a classical limit of the original many-electron system. Hereafter we refer to the classical limit of the QFM as the classical oscillator model (COM). As shown in [22] any classical system can be mapped onto a set of classical coupled oscillators.

(ii) In the vicinity of the stationary solution $\rho^{gg} \in M$ of the TDHF equation we transform the local variables on $\mathbf{M}$ so that the Poisson bracket assumes a canonical form. This establishes the oscillator representation of the COM. Stated differently, this shows the equivalence of the COM and a classical canonical oscillator model (CCOM) defined as the COM represented in terms of the canonical variables.

(iii) We build the quantum oscillator model (QOM) by quantizing the CCOM, so that the classical limit of the QOM reproduces the CCOM. The classical system of oscillators can therefore be viewed as the classical limit of a system of quantum coupled oscillators. We thus have two quantum models: QFM which corresponds to the original electronic system, and the system of quantum anharmonic oscillators (QOM). Their classical limits COM and CCOM respectively are equivalent, and the COM describes the QFM within the TDHF approximation.
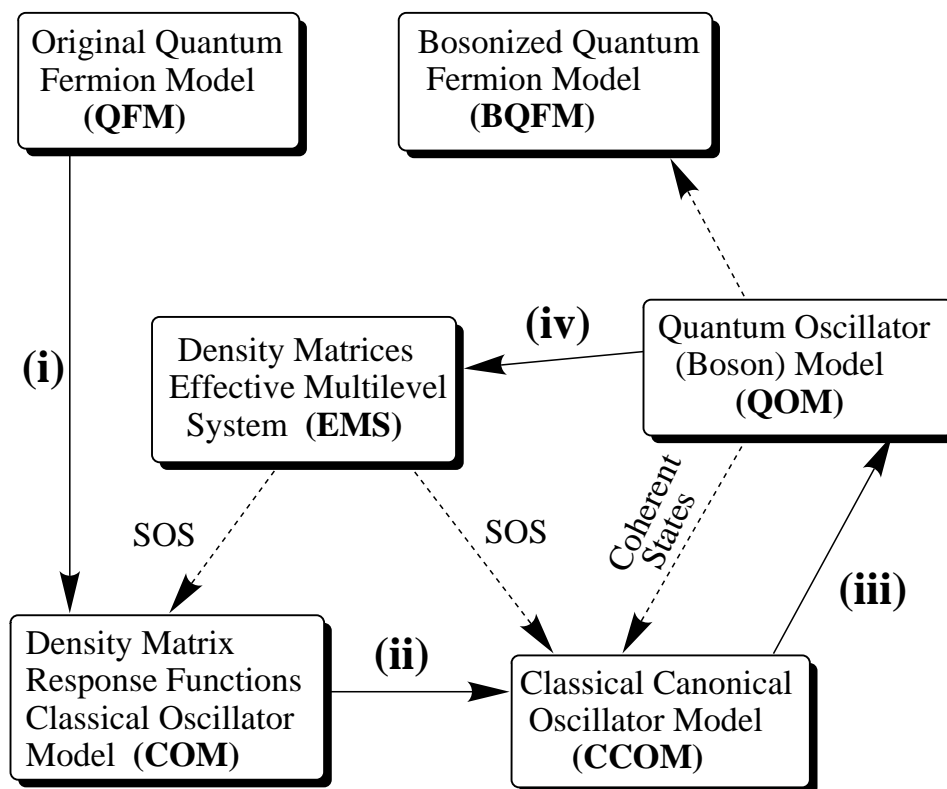
FIG. 1. The four steps involved in constructing the effective multilevel system (EMS)out of the original quantum Fermion Model (QFM). Obtaining a Bosonized Quantum Fermion Model (BQFM) out of the quantum oscillator model should allow to reproduce the exact density matrix response functions, and not rely on the TDHF. This extension goes beyond the scope of the present work.

(iv) Finally, using a perturbative approach we build an effective multilevel system (EMS) whose exact optical response reproduces the classical approximation of the QOM which is the CCOM and in turn coincides with the TDHF approximation of the original model QFM. In summary, the EMS constitutes a quantum model whose optical response reproduces the TDHF approximation of the original model.

In Section II we carry out steps (i) and (ii) and map the original quantum fermion model onto a classical canonical oscillator model. Steps (iii) and (iv) are made in Section III. Computational details are given in the Appendices. In Section IV we apply this algorithm to a family of unsubstituted and acceptor-substituted carotenoids. The induced density matrices $\rho_{nm}^{\nu\eta}$ for the states which dominate the linear and the quadratic response are investigated. Finally we discuss and summarize our results in Section V.

II. THE TDHF APPROACH: CLASSICAL ELECTRONIC OSCILLATORS

We consider a system described by the molecular electronic Hamiltonian [14,23].

$$\widehat{H} = \sum_{mn\sigma} t_{mn} c_{m\sigma}^+ c_{n\sigma} + \sum_{\substack{mnkl \\ \sigma\sigma'}} \langle nm|kl \rangle c_{m\sigma}^+ c_{n\sigma'}^+ c_{k\sigma'} c_{l\sigma} - \mathcal{E}(t) \sum_{mn\sigma} \mu_{mn} c_{m\sigma}^+ c_{n\sigma}, \qquad (2.1)$$

where $c_{m,\sigma}^+ (c_{m,\sigma})$ are the annihilation (creation) operators of an electron on atomic orbital m with spin σ which satisfy the Fermi anticommutation relations (assuming an orthogonal basis set)

$$c_{m\sigma}c_{n\sigma'}^+ + c_{n\sigma'}^+ c_{m\sigma} = \delta_{mn}\delta_{\sigma\sigma'}, \tag{2.2}$$

and all other anticommutators of c^+ and c vanish. $\hat{\rho}_{nm}^\sigma = c_{m,\sigma}^+ c_{n,\sigma}$ is the reduced single-electron density operator [14–17]. The first term in Eq. (2.1) is the single-electron (core) hamiltonian describing the kinetic energy and nuclear attraction of an electron, the second term represents electron-electron (Coulomb) interactions where $\langle mk|nl\rangle$ are the two-electron integrals, and the last term gives the interaction between the electrons and the external electric field $\mathcal{E}(\mathbf{t})$, μ being any single-electron operator [21,23].

The classical oscillator model is constructed using the procedure for approaching the classical limit outlined in [22]. We start by defining the phase space of the single Slater determinants $\mathbf{M}$ (defined up to a phase) known as the Grassman manifold $G(M,N;C)$, N being the basis set size and M is the number of electrons. The Grassman manifold $\mathbf{M} = G(M,N;C)$ can be alternatively represented as the space of hermitian $N \times N$ single-electron reduced density-matrices with $\rho^2 = \rho$ and rank$(\rho) = M$. The classical Hamiltonian is given as

$$H(\rho) = \langle \Omega(\rho)|\widehat{H}|\Omega(\rho)\rangle, \tag{2.3}$$

where $\Omega(\rho)$ is the Slater determinant corresponding to ρ. Expressions for $H(\rho)$ in terms of the original parameters of the molecular electronic Hamiltonian (Eq. (2.1)) and for the Poisson bracket were given in [21]. The TDHF equation adopts the form of the equation of motion of Hamilton's classical dynamics on $\mathbf{M}$. The stationary point of the TDHF equations which corresponds to the minimum of the energy function $H(\rho)$ on $\mathbf{M}$ constitutes the Hartree-Fock (HF) reduced ground state single-electron density matrix ρ^{gg} which can be found by solving the Hartree-Fock (HF) equation [14]

$$[F(\rho^{gg}),\rho^{gg}] = 0, \tag{2.4}$$

where $F(\rho^{gg})$ is the Fock matrix

$$F(\rho^{gg}) = t + V(\rho^{gg}), \tag{2.5}$$

and the matrix elements of the Coulomb electronic operator V are

$$V(\rho^{gg})_{mn} = \sum_{k,l} \rho_{kl}^{gg}[\langle mk|nl\rangle - \frac{1}{2}\langle mn|kl\rangle]. \tag{2.6}$$

To construct the classical oscillators (step (ii)) we need to define local coordinates on $\mathbf{M}$ representing deviations from ρ^{gg}. The restricted TDHF scheme [21] allows us to reduce the number of variables from N^2 to particle-hole variables $M(N-M)$ only. To that end we decompose the single-electron density matrix in the form

$$\rho = \rho^{gg} + \xi + T(\xi). \tag{2.7}$$

Here ξ represents the particle-hole whereas $T(\xi)$ is the particle-particle and the hole-hole parts of the deviation of the reduced single-electron density matrix from the ground state ρ^{gg}. ρ^{gg}, ξ, and $T(\xi)$ in Eq. (2.7) are $N \times N$ matrices. [1] The particle-particle and hole-hole components of the density matrix are not independent variables, since they can be expressed in terms of the particle-hole part [21,23]. Therefore only the particle-hole components of the density matrix, ξ, need to be calculated explicitly. T can be expanded in a Taylor series which contains only even powers of ξ. For computing DMRF not higher than third order it is sufficient to retain only the lowest (second order) term [21,23].

$$T(\xi) = \frac{1}{2}[[\xi, \rho^{gg}], \xi] = (I - 2\rho^{gg})\xi^2. \tag{2.8}$$

where I is the $N \times N$ unit matrix.

A convenient coordinate system can be introduced by parameterizing the electron-hole component (ξ) of the density matrix. To introduce variables close to canonical (as will be explained latter) it is convenient to use the TDHF equations for $\xi(t)$:

$$i\frac{\partial}{\partial t}\xi(t) = L(\xi) - \mathcal{E}[\mu, \rho] + [V(\xi), \xi + T(\xi)] + [V(T(\xi)), \xi + \rho^{gg}] , \tag{2.9}$$

where ρ is given by Eq. (2.7) and the Liouville space operator (superoperator) L represents the linear part of the equation [21,23]

$$L(\xi) = [t + V(\rho^{gg}), \xi] + [V(\xi), \rho^{gg}] \quad . \tag{2.10}$$

The oscillator variables are computed as the eigenmodes of the linear part of Eq. (2.9) satisfying:

$$L(\xi_\alpha) = \Omega_\alpha \xi_\alpha, \quad L(\xi_{-\alpha}) = -\Omega_\alpha \xi_{-\alpha} \quad . \tag{2.11}$$

These oscillators are orthonormal:

$$\mathrm{Tr}(\rho^{gg}[\xi_{-\alpha}, \xi_\beta]) = \delta_{\alpha,\beta} \quad . \tag{2.12}$$

and the particle-hole part of the density matrix can be expanded in ξ_α [21,23]

$$\xi(t) = \sum_{\alpha>0} z_\alpha(t)\xi_\alpha + z_\alpha^*(t)\xi_\alpha^+ \quad . \tag{2.13}$$

Each oscillator α is described by two complex operators ξ_α and ξ_α^+. Following the notation of Ref. [21] we define $\xi_{-\alpha} = \xi_\alpha^+$. z_α and its complex conjugate $z_{-\alpha} = z_\alpha^*$ constitute the complex oscillator amplitudes. A classical picture is obtained by introducing the oscillator coordinates $Q_\alpha \equiv \frac{1}{\sqrt{2}}(\xi_\alpha + \xi_\alpha^+)$ and the momenta $P_\alpha \equiv \frac{i}{\sqrt{2}}(\xi_\alpha - \xi_\alpha^+)$ [21]. However, it is more convenient to keep the complex ξ_α variables

Eqs. (2.13) and (2.7) define a local coordinate system z_α on $\mathbf{M}$ where ρ^{gg} is the origin. Substitution of Eqs. (2.13) and (2.7) into Eq. (2.3) yields the classical Hamiltonian for the variables z_α. $H(z_\alpha)$ can be calculated in a form of an expansion in powers of z_α. The

---

[1] ρ^{gg} and $\xi(t)$ are matrices of rank M, $M < N$.

expression to fourth-order is presented in [21]. For the applications made in this paper we only need the Hamiltonian up to third-order

$$H(z) = \sum_{\alpha > 0} \Omega_\alpha z_{-\alpha} z_\alpha + \frac{1}{3} \sum_{\alpha\beta\gamma} V_{\alpha,\beta\gamma} z_\alpha z_\beta z_\gamma - \mathcal{E}(t) \mathcal{P}(z) \ , \tag{2.14}$$

with the polarization

$$\mathcal{P}(z) = \sum_\alpha \mu_\alpha z_\alpha + \frac{1}{2} \sum_{\alpha\beta} \mu_{\alpha\beta} z_\alpha z_\beta \ , \tag{2.15}$$

where

$$\mu_\alpha = \mathrm{Tr}([\rho^{gg}, \xi_\alpha][\mu, \rho^{gg}]) \tag{2.16a}$$

$$\mu_{\alpha,\beta} = \mathrm{Tr}([\rho^{gg}, \xi_\alpha][\mu, \xi_\beta]) \tag{2.16b}$$

$$V_{\alpha,\beta\gamma} = \mathrm{Tr}([\rho^{gg}, \xi_\alpha][V(\xi_\beta), \xi_\gamma])$$
$$+ \mathrm{Tr}([\rho^{gg}, \xi_\alpha][V(\frac{1}{2}[[\xi_\beta, \rho^{gg}], \xi_\gamma]), \rho^{gg}]). \tag{2.16c}$$

All quantities here are $N \times N$ matrices in the single-electron space, and the trace is defined in this space.

The Poisson bracket for the z_α variables is calculated in [21] and to first-order in z_α it has the canonical form

$$\{z_\alpha, z_\beta\} = i\delta_{\alpha,-\beta} \ . \tag{2.17}$$

It has the following useful properties:

$$\{z_\alpha, z_\beta\} = -\{z_\beta, z_\alpha\} \ , \tag{2.18}$$

$$\{z_\alpha, z_\beta z_\gamma\} = \{z_\alpha, z_\beta\} z_\gamma + z_\beta \{z_\alpha, z_\gamma\} \ . \tag{2.19}$$

The classical Hamilton equation of motion $\dot{z} = \{H, z\}$ obtained using Eqs. (2.14)-(2.16) can be written as

$$i\frac{\partial}{\partial t} z_\alpha = \Omega_\alpha z_\alpha - \mathcal{E}\mu_{-\alpha} - \mathcal{E} \sum_\beta \mu_{-\alpha,\beta} z_\beta + \sum_{\beta\gamma} V_{-\alpha,\beta\gamma} z_\beta z_\gamma \quad . \tag{2.20}$$

These equations are equivalent to Eq. (2.9). The linear and the second order response functions calculated by solving these equations are given in Appendix A.

Eqs. (2.14)-(2.20) define the classical oscillator model. The variable z_α describes the α'th oscillator, as is clearly seen from the form of the Poisson bracket [Eq. (2.16)]. Higher-order terms of the Hamiltonian can be calculated order-by-order. Similarly, the Poisson bracket is not strictly canonical and the r.h.s. of Eq. (2.17) can be expanded in powers of z_α. Second order corrections have been calculated in [22]. These deviations can however be eliminated since the Poisson bracket can be always transformed to a canonical form [24] using a nonlinear transformation of variables

$$z'_\alpha = z_\alpha + \sum_{\alpha\beta\gamma\delta} S_{\alpha,\beta\gamma\delta} z_\beta z_\gamma z_\delta + \dots \ . \tag{2.21}$$

In practice, the canonical variables can be calculated order-by-order in z_α. Expressing the Hamiltonian in terms of the canonical variable z'_α allows us to define a CCOM to any given order in z_α. This accomplishes step (ii) of the procedure.

III. INTRASTATE AND TRANSITION ELECTRONIC DENSITY MATRICES FOR THE EFFECTIVE MULTILEVEL SYSTEM

Steps (iii) involves the construction of a quantum oscillator model QOM whose classical limit reproduces the CCOM. To that end we associate with each classical variable z_α an annihilation operator a_α ($z_\alpha = \langle a_\alpha \rangle$, $\alpha > 0$), $z_{-\alpha} = z_\alpha^*$ is associated with a creation operator a_α^+ ($z_\alpha^* = \langle a_\alpha \rangle^+$). These satisfy the boson commutation relations:

$$[a_\alpha, a_\beta^+] = \delta_{\alpha\beta} . \tag{3.1}$$

We define the QOM Hamiltonian H_1 by

$$H_1 =: H(a_\alpha, a_\alpha^+) : , \tag{3.2}$$

where $H(a_\alpha, a_\alpha^+)$ is the classical Hamiltonian of the CCOM, which is given by Eqs. (2.14) and (2.15) up to third order, and $:\ldots:$ stands for normal ordering. We then have

$$H_1 = \sum_\alpha \Omega_\alpha a_\alpha^+ a_\alpha + \frac{1}{3!} \left(\sum_{\alpha\beta\gamma} V_{\alpha,\beta\gamma} a_\alpha a_\beta a_\gamma + 3 \sum_{\alpha\beta\gamma} V_{-\alpha,\beta\gamma} a_\alpha^+ a_\beta a_\gamma + h.c. \right) - \mathcal{E}\mathcal{P}(a_\alpha^+, a_\alpha) , \tag{3.3}$$

with

$$\mathcal{P}(a_\alpha^+, a_\alpha) = \sum_\alpha \mu_\alpha a_\alpha + \frac{1}{2!} \left(\sum_{\alpha\beta} \mu_{\alpha\beta} a_\alpha a_\beta + \sum_{\alpha\beta} \mu_{-\alpha\beta} a_\alpha^+ a_\beta + h.c. \right) , \tag{3.4}$$

and the summation in Eqs. (3.3) and (3.4) runs over $\alpha, \beta, \gamma > 0$.

The classical limit of the QOM can be obtained by requiring that each oscillator α remains in a coherent state parameterized by z_α at all times. This amounts to the following factorizations $\langle a_\alpha a_\beta \rangle = z_\alpha z_\beta$ and $\langle a_\alpha^+ a_\beta \rangle = z_\alpha^* z_\beta$. Using these factorizations, the Heizenberg equation of motion $\dot{a}_\alpha = \frac{i}{\hbar}[H_1, a_\alpha]$ with H_1 given by Eq. (3.3) coincides with the classical equation of motion (Eq. (2.20)). The CCOM is thus the classical limit of the QOM and step (iii) is accomplished.

We turn now to step (iv), namely constructing the effective multilevel system EMS whose response reproduces the classical limit of QOM (which, in turn, coincides with the TDHF approximation of the QFM). This will be based on the picture established in [22] that the semiclassical expansion is a reexpansion of the optical response in the anharmonicities of the Hamiltonian and nonlinearities of the polarization operator in a and a^+. This is carried out for the response up to second order in Appendix B. In particular, the linear response in the classical approximation is obtained by setting $V_{\alpha,\beta\gamma} = 0$ and $\mu_{\alpha\beta} = 0$ (i.e., using the model of a set of linearly driven uncoupled harmonic oscillators) whereas the second-order response also depends on the terms proportional to $V_{\alpha,\beta\gamma}$ and $\mu_{\alpha\beta}$.

The QOM is improved successively by incorporating higher-order responses. We will concentrate on the lower-energy excited states which can be constructed using the linear and the second-order responses. For the linear response we set $V_{\alpha,\beta\gamma} = 0$ and $\mu_{\alpha\beta} = 0$ and obtain a system of harmonic oscillators with the polarization linear in a and a^+. Since the polarization is represented by the most general operator given by linear and bilinear

combinations $c_m^+ c_n$ of fermion operators, we can obtain the matrix elements of $c_m^+ c_n$ between the ground state and single-excited oscillator states involved in the linear response. The second order response depends on the anharmonicities to the first order. This leads to first-order corrections to the oscillator wavefunctions whereas the eigenvalues remain the same (since they only contain higher-order corrections). This implies that in this order of perturbation theory which corresponds to the classical limit, the system remains harmonic and simply attains new matrix elements of $c_m^+ c_n$.

It follows from Eqs. (2.1) and (3.3) together with Eqs. (2.16) that the operator $c_m^+ c_n$ can be represented in terms of the oscillator operators in the following form

$$
c_m^+ c_n = \rho_{mn}^{gg} + \sum_\alpha \left\{ (\xi_\alpha^+)_{mn} a_\alpha^+ + (\xi_\alpha)_{mn} a_\alpha \right\} + \frac{1}{2} \sum_{\alpha\beta} \left\{ ([\xi_\alpha^+, \rho^{gg}]\xi_\beta^+])_{mn} a_\alpha^+ a_\beta^+ \right.
$$

$$
\left. + ([\xi_\alpha^+, \rho^{gg}]\xi_\beta])_{mn} a_\alpha^+ a_\beta + ([\xi_\alpha, \rho^{gg}]\xi_\beta^+])_{mn} a_\alpha a_\beta^+ + ([\xi_\alpha, \rho^{gg}]\xi_\beta])_{mn} a_\alpha a_\beta \right\} . \quad (3.5)
$$

The EMS is constructed as a system of harmonic oscillators with the eigenstates $|k\alpha, l\beta, \ldots\rangle$ and eigenenergies $E = k\Omega_\alpha + l\Omega_\beta + \ldots$, where the integers $k, l = 0, 1, 2, \ldots$ label the excited states of the various oscillators. The EMS are calculated to first-order in V in terms of the oscillator states of QOM in Appendix B. The contributions to the response functions $S^{(j)}$ can, therefore, be classified according to the matrix elements of the effective oscillator system $\langle k\alpha, \ldots | c_m^+ c_n | l\beta, \ldots \rangle$.

The effective level scheme that reproduces the linear response $S^{(1)}$ (Eq. (A3) consists of the ground state $|g\rangle$ and all single excitations $|1\alpha\rangle$. The relevant density matrix elements are

$$
\langle g | c_m^+ c_n | g \rangle = \rho_{mn}^{gg} , \quad (3.6a)
$$

$$
\langle g | c_m^+ c_n | 1\alpha \rangle = (\xi_\alpha)_{mn} . \quad (3.6b)
$$

Eqs. (3.6a) and Eq. (3.6b) simply recover our input i.e. the ground state density matrix and the TDHF electronic modes contributing to the linear response.

The second-order response $S^{(2)}$ (Eq. (A4) is represented by an effective system consisting of the ground state $|g\rangle$, single $|1\alpha\rangle$, and double $|1\alpha 1\beta\rangle$ excited states. These are given by Eqs. (B3) to first order in V. (The state $|2\alpha\rangle$ is the special case of $|1\alpha 1\beta\rangle$ when $\alpha = \beta$.) The necessary additional matrix elements are obtained by combining Eqs. (B3) and (3.5):

$$
\langle g | c_m^+ c_n | 1\alpha 1\beta \rangle = \frac{([\xi_\alpha, \rho^{gg}]\xi_\beta])_{mn}}{2} + 2 \sum_\gamma \left\{ \frac{V_{\alpha\beta-\gamma}(\xi_\gamma)_{mn}}{\Omega_\alpha + \Omega_\beta - \Omega_\gamma} - \frac{V_{\alpha\beta\gamma}(\xi_\gamma^+)_{mn}}{\Omega_\alpha + \Omega_\beta + \Omega_\gamma} \right\} , \quad (3.7a)
$$

$$
\langle 1\alpha | c_m^+ c_n | 1\beta \rangle = \rho_{mn}^{gg} \delta_{\alpha\beta}
$$

$$
+ ([[\xi_\alpha^+, \rho^{gg}]\xi_\beta])_{mn} + \sum_\gamma \left\{ \frac{V_{-\alpha-\beta\gamma}(\xi_\gamma)_{mn}}{-\Omega_\alpha + \Omega_\beta - \Omega_\gamma} + \frac{V_{\alpha\beta-\gamma}(\xi_\gamma^+)_{mn}}{\Omega_\alpha - \Omega_\beta - \Omega_\gamma} \right\} , \quad (3.7b)
$$

$$
\langle 1\alpha | c_m^+ c_n | 1\beta 1\gamma \rangle = (\xi_\gamma)_{mn} \delta_{\alpha\beta} + (\xi_\beta)_{mn} \delta_{\alpha\gamma} , \quad (3.7c)
$$

where $V_{\alpha\beta\gamma}$ is given by Eq. (2.16c).

Eq. (3.7a) gives transition density matrices involving the ground state. Eq. (3.7b) expresses the transition density matrices between singly-excited states obtained from $S^{(1)}$, and

Eq. (3.7c) gives the transitions between singly and doubly excited states. The first term in Eqs. (3.7a) and (3.7b) represents the interband (particle-particle and hole-hole) part of the density matrix, and involves only two electronic modes. The second (intraband, particle-hole and hole-particle) term, involves a summation over all electronic modes. These matrices provide an approximation for the density matrices between states contributing to the first- and to the second-order optical responses. The corresponding energies are

$$\Omega_{1\alpha} = \Omega_\alpha; \qquad \Omega_{1\alpha1\beta} = \Omega_\alpha + \Omega_\beta \ . \tag{3.8}$$

Taking higher order anharmonicities into account will allow us to compute density matrix elements involving new states. For example, the third-order response $S^{(3)}$ includes higher lying excitations: $\langle g|c_m^+c_n|1\alpha1\beta1\gamma\rangle$, $\langle 1\alpha|c_m^+c_n|1\beta1\gamma1\delta\rangle$, $\langle 1\alpha1\beta|c_m^+c_n|1\gamma1\delta1\zeta\rangle$, $\langle 1\alpha1\beta|c_m^+c_n|1\gamma1\delta\rangle$. In general, $S^{(j)}$ involves all transitions contributing to the lower order responses, j-transitions from the ground, single, double, ..., $(j-1)$th excited states to the j'th excited state, and transitions between $(j-1)$th excited states.

By using an arbitrary single-particle operator μ_{mn} in Eqs. (3.7) we can compute the full density matrix response function, which depends on all electronic modes. When μ_{mn} is taken to be the dipole operator, we only obtain those modes that dominate the optical response. The ability to focus on the dominant modes alone has proved to be very useful for calculating the optical response [23,26–29]. However, in order to compute the excited-state density matrices we need to capture all the modes (optically bright and dark).

When only few modes are known, Eqs. (3.7a) and (3.7b) are dominated by the interband term $([\xi_\alpha, \rho^{gg}]\xi_\beta)$. The summation over available modes gives a negligible contribution because, in general, $V_{\alpha\beta\gamma} \ll 1$. The resulting transition matrices ($\langle 1\alpha|c_m^+c_n|1\beta\rangle$, $\langle g|c_m^+c_n|1\alpha1\beta\rangle$) will, therefore, preserve all localization properties of the ground state ρ^{gg} and electronic modes ξ_α and ξ_β. On the other hand, the summation over all TDHF modes significantly increases the contribution of the second term in Eqs. (3.7a) and (3.7b) yielding the transition matrices which do not depend on the way the molecule interacts with the optical field (molecular dipole) but represent intrinsic molecular properties.

IV. DENSITY MATRICES OF ACCEPTOR-SUBSTITUTED CAROTENOIDS.

We have applied the present algorithm to a family of symmetric nonpolar (N) and polar (P) conjugated polyenes whereby one end is substituted with a strong acceptor group (see Fig. 2). The linear absorption and the electronic modes responsible for the optical response of these molecules were studied in [23,25]. The Hartree-Fock ground-state density matrices were calculated first. Optimal ground-state geometries were obtained at the AM1 level using Gaussian-94. The ZINDO code was utilized to generate INDO/S [30–32] hamiltonian, and the collective electronic oscillator (CEO) procedure [23,26,28] was then applied to compute the dominant electronic modes and the corresponding dipole moments $\mu_\nu^{(j)}$ which contribute to the first and to the second order off-resonant optical response:[2]

---

[2]INDO/S hamiltonian was initially parameterized to reproduce electronic spectra at CIS level. However, we found that it works also extremely well without further reparameterization with
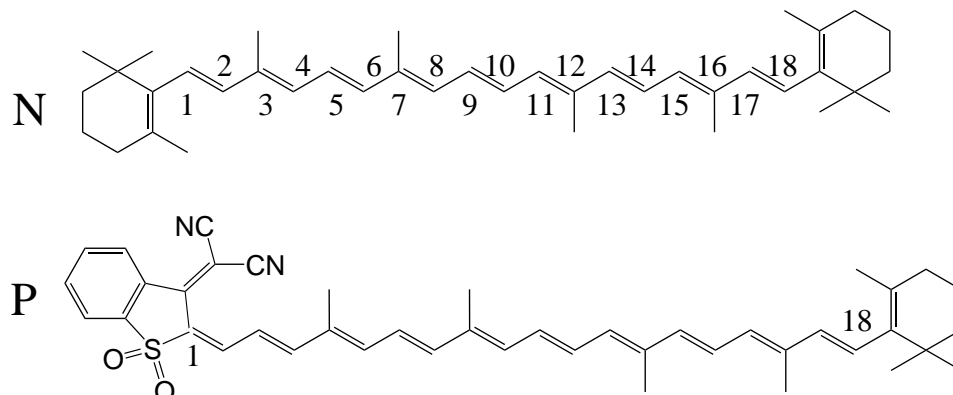
FIG. 2. Structures and atom labeling of the neutral N and polar P (substituted by the strong acceptor) molecules.

$$\xi^{(j)} = \sum_{\nu} \mu_{\nu}^{(j)} \xi_{\nu} + (\mu_{\nu}^{(j)})^* \xi_{\nu}^+ , \quad j = 1, 2 . \tag{4.1}$$

Satisfactory convergence of the response to within $\sim 10^{-3}$ was achieved using 10-15 effective electronic modes.

In Figure 3 we display the dipole moments (Eq. (4.1)) of the dominant modes vs. mode frequencies Ω_{ν}, calculated using the first and the second order response. Since the N molecule has an inversion symmetry, the first-order response depends only on antisymmetric (B_u) oscillators (panel A) whereas the second-order response depends on symmetric (A_g) oscillators (panel B). The figure shows that the response of the N molecule is dominated by a single electronic mode. In contrast, the P molecule shows four major peaks in each order of the response, and its electronic oscillators do not possess any symmetry. The same modes (a and b) with different dipoles show up in both responses.

We next examine the single-electron density matrices $\rho_{nm}^{\nu\eta}$ for the states corresponding to peaks a, b, and c in N and a' b', c' and d' in P. These density matrices computed using Eqs. (3.6) and (3.7) represent the projection of the full matrix which contributes to the first and to the second order response, because only the electronic modes which dominate the linear and the quadratic optical responses were used in the calculations. Other components of the matrix do not have a dipole moment and, therefore, do not contribute to the optical response. The acceptor's effect on the molecular properties can be illustrated using contour plots of the density matrices. The absolute value of the reduced ground state density matrix ρ^{gg} of N is shown in the upper left panel of Fig. (4). The axes represent carbon atoms. The ground state density matrix is dominated by diagonal and near-diagonal elements, reflecting

---

the CEO for a broad range of molecules: Computed linear absorptions of acceptor-substituted carotenoids [23], stilbenoid aggregates [33], phenylacetylene dendrimers [28], porphins [34,35], and static second-order polarizabilities of donor/acceptor substituted polyenes [29] compared well with experiment. The input to these calculations, the ground-state structures, could be obtained using other semiempirical (e.g. AM1), *ab initio* optimized molecular geometries, experimental X-ray diffraction, or NMR data. The issue of optimizing INDO/S hamiltonian parameters for the CEO approach or using other hamiltonians is an open problem that lies beyond the scope of current paper
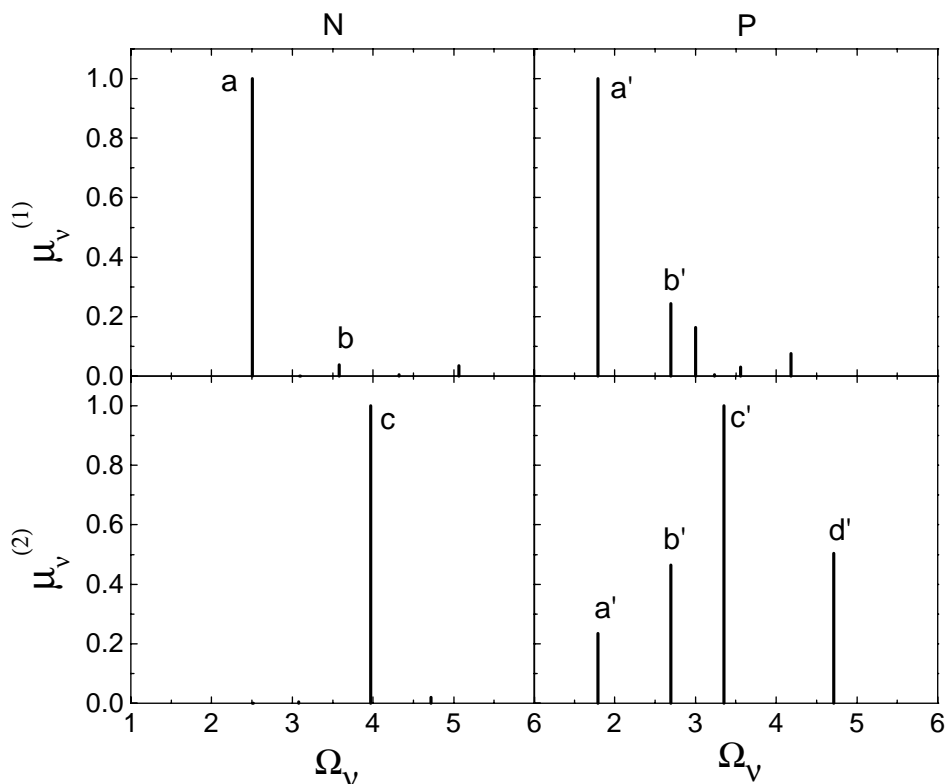
FIG. 3. The dipole moments μ_ν are displayed vs. electronic mode frequencies Ω_ν for the molecules shown in Fig. 2. Shown are the dominant modes in the first two orders of nonlinearity. The dipoles are given in arbitrary units.

the bonds between nearest neighbors. The (x1) scaling factor indicates that the largest values of the matrix shown by the blue color are equal to 1. The diagonal elements represent the electronic charges on each carbon atom. The absolute values of the matrix $\Delta\rho^{aa} \equiv \rho^{aa} - \rho^{gg}$ (panel $N(\rho^{aa})$) is the difference between the density matrix of state a and the ground state density matrix. The matrix is delocalized over the entire molecule. The x10 factor implies that the part of the excited state density matrix which contributes to the second-order optical response only changes slightly compared to the ground state. The difference for the density matrix of state b $\Delta\rho^{bb}$ (panel $N(\rho^{bb})$) is less delocalized compared with $\Delta\rho^{aa}$. In addition it is nonuniform along the diagonal, which leads to diagonal localization sizes. $\Delta\rho^{cc}$ corresponding to the electronic mode contributing to the second-order optical response possesses a delocalization and magnitude similar to $\Delta\rho^{aa}$. For all excited state matrices, the off-diagonal elements are much larger than the diagonal. This means that upon optical excitation of the unsubstituted molecule the changes in the bonding pattern are much more significant compared with the charge redistribution.

The transition density matrices are displayed in the middle and the right columns of Fig. (4). Transitions involving the ground state are described by the electronic modes (ρ^{ga}, ρ^{gb}, and ρ^{gc}). Their role in the optical response has been analyzed in [23]; They have delocalization properties very similar to the corresponding states density matrices, because in the calculations of the latter these modes make the dominant contribution. Similarly, the transition density matrices between excited states shown in the right column of Fig. (4)
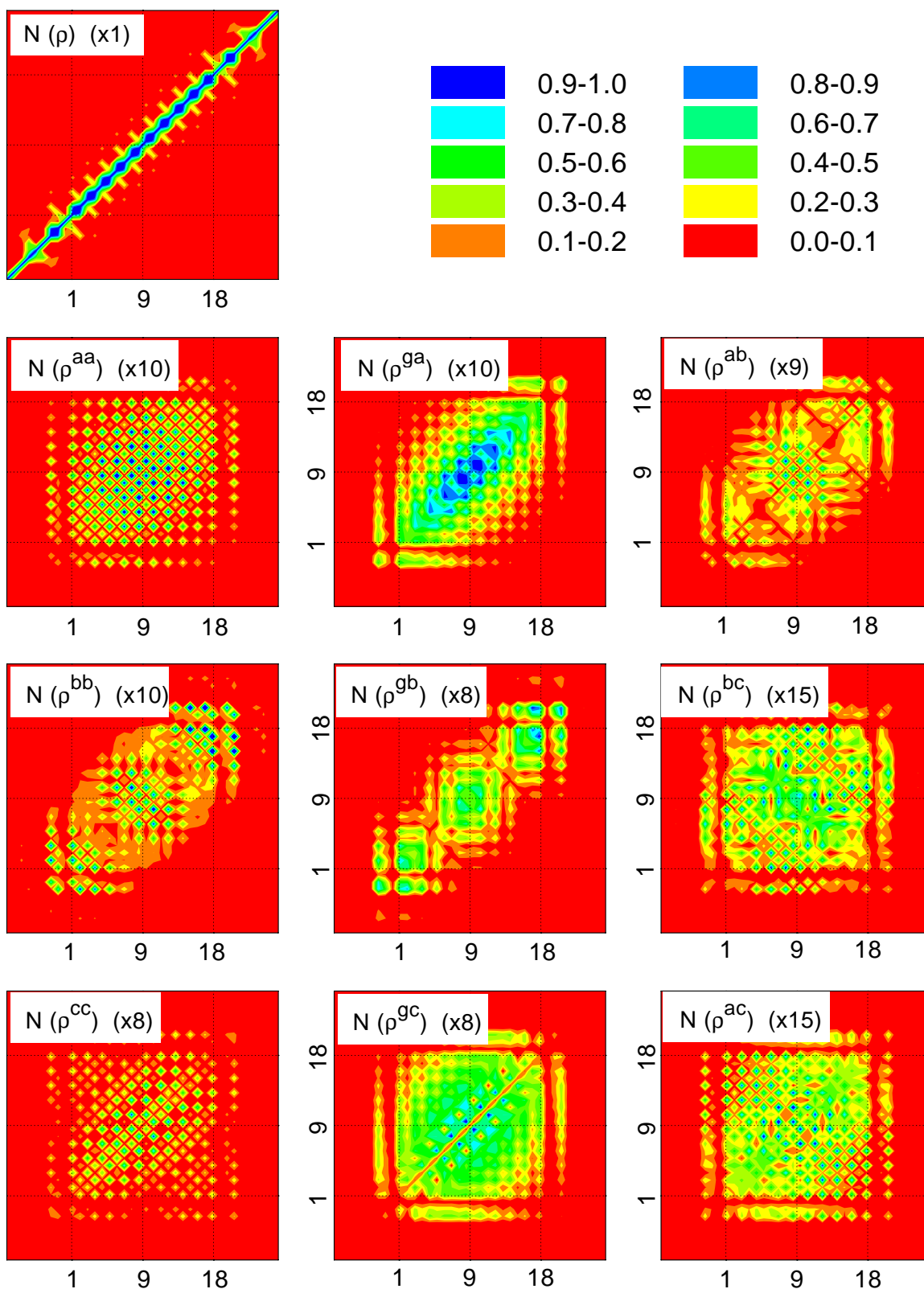
FIG. 4. Contour plots of ground and excited state density matrices which dominate the linear absorption of molecules N. The axis labels represent the individual carbon atoms as labeled in Fig. 2. Panel labels indicate the molecule (Fig. 2) and the state corresponding to the peak in Fig. 3. ρ^{gg} ground state density matrix; $\Delta\rho^{\nu\nu} \equiv \rho^{\nu\nu} - \rho^{gg}$ the difference between the density matrices of state ν and the ground state; $\rho^{\nu\eta}$ the transition density matrices.
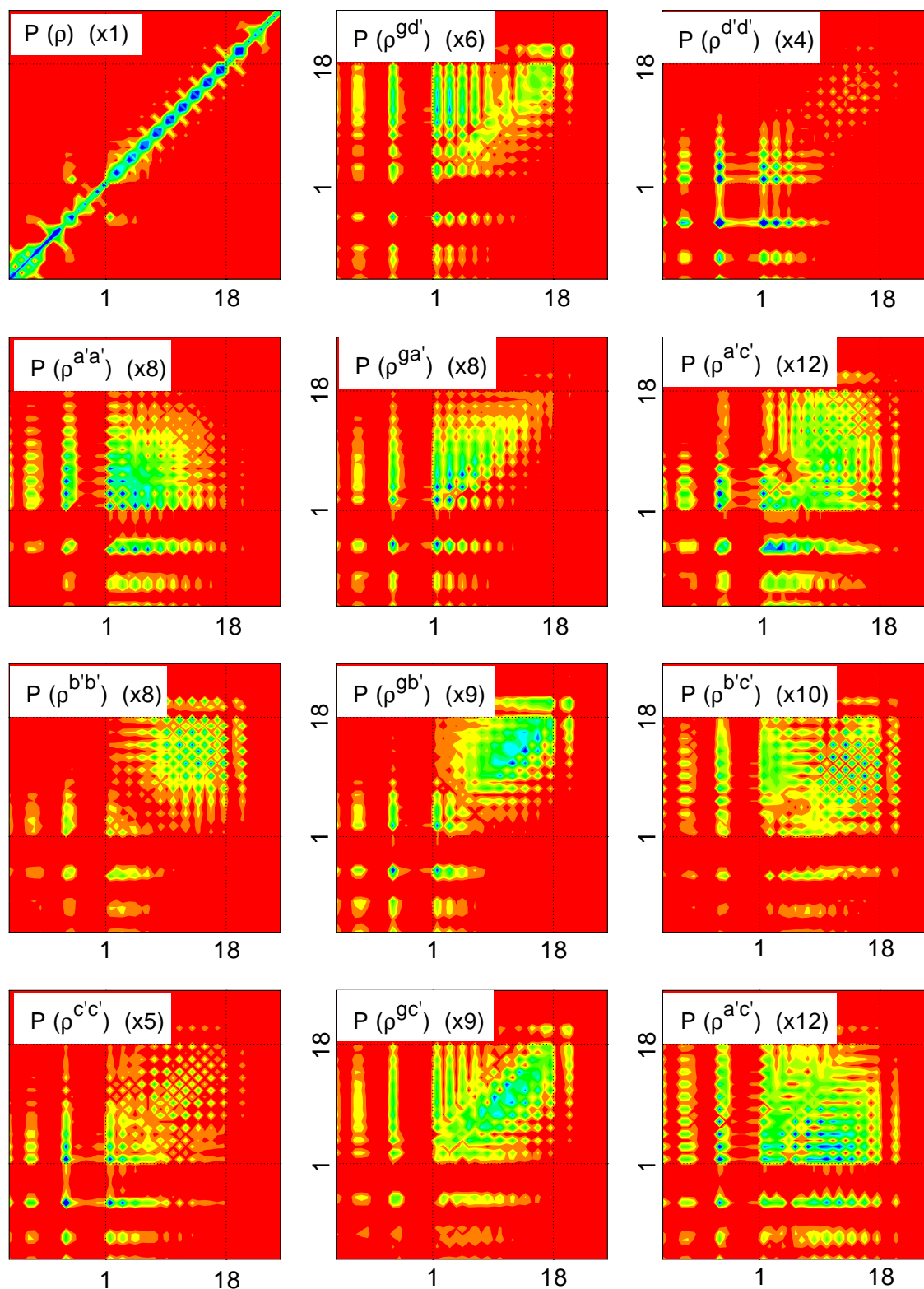
FIG. 5. Same as in Fig. 4 but for the polar molecule P.

are symmetric and delocalized over the entire molecule. The largest coherences appear to be at the center of the matrices because the density matrices of states a, b, and c have the strongest bonding pattern at the center.

Fig. (5) displays the absolute values of the calculated density matrices of P. The strong acceptor perturbs the ground state, as shown by the reduction of the electronic density towards the acceptor in panel P ρ^{gg}. The difference $\Delta\rho^{a'a'}$ for state a' is localized in the acceptor end (panel P($\rho^{a'a'}$)), whereas $\Delta\rho^{b'b'}$ for state b is localized on the neutral end of the molecule (panel P($\rho^{b'b'}$)). Note that $\Delta\rho^{a'a'}$ has very large diagonal and off-diagonal elements implying that excitation to state a changes the charge distribution as well as the bonding pattern compared to the ground state. In contrast, $\Delta\rho^{b'b'}$ is dominated by off-diagonal elements, which makes it similar to the excited state density matrices of the unsubstituted molecule. This reflects the fundamental difference between states a' and b'. $\Delta\rho^{c'c'}$ and $\Delta\rho^{d'd'}$ corresponding to the electronic mode contributing to the second-order optical response are both localized at the acceptor end, and are dominated by a few large diagonal and off-diagonal elements. The former has a stronger bulk contribution.

The transition density matrices between the ground and the excited states (electronic modes $\rho^{ga'}$ and $\rho^{gb'}$) are highly asymmetric and delocalized, reflecting the motions of charges along the molecule upon optical excitation. The x and the y axis label the electron and the hole respectively. The diagonal elements ρ_{nn} show induced charges on various atoms whereas the off-diagonal elements ρ_{nm} represent the probability amplitude of finding an excess electron at the m-th atomic orbital and a hole on the n-th atomic orbital. $\rho^{gc'}$ and $\rho^{gd'}$ corresponding to the high frequency excited states and contributing to the second order response are less asymmetric than the former and delocalized over the entire molecule (compared with $\rho^{c'c'}$ and $\rho^{d'd'}$). The transition density matrices shown in the right column of Fig. (5) are delocalized over the entire molecule. The largest coherences appear where the density matrices of corresponding states have the strongest bonding patterns. Note that these density matrix elements are smaller (x10-12) compared to the other displayed matrices (x4-9), because the states a, b', and c' are localized in different regions.

V. DISCUSSION

The TDHF uses the single-electron density matrix $\langle g|c_m^+ c_n|g\rangle$ to calculate the single-electron transition density matrices (electronic modes) between the ground state and the excited electronic states $\langle g|c_m^+ c_n|1\alpha\rangle$ which contribute to the linear response. In this article we made one step further: using the ground-state density matrix and the electronic modes we calculated additional density matrices: between the ground state and the excited states $\langle g|c_m^+ c_n|1\alpha 1\beta\rangle$ which contribute to the second-order response, transition density matrices between states $\langle 1\alpha|c_m^+ c_n|1\beta\rangle$ as well as the single-electron density matrices of the excited states $\langle 1\alpha|c_m^+ c_n|1\alpha\rangle$ which contribute to the linear response.

The TDHF procedure maps the quantum many-electron system onto a system of classical oscillators. The present approach is based on inverting the optical response function and mapping the original system onto an effective set of quantum states. An algorithm is developed for calculating Density-Matrix-Response-Functions (DMRF) for excited electronic states using the Time-Dependent Hartree-Fock (TDHF) approximation. The DMRF carries additional excited-state information about charge distributions and bonding patterns as well as the dynamical changes induced in these quantities by the external field.

The present analysis has several advantages. First, it connects the TDHF representation with the quantum-mechanical treatments of the optical response in terms of global many-electron eigenstates. The latter may be useful for representing the properties of optically excited molecule. The procedure is further numerically inexpensive. The absence of long range electronic coherence may be used to reduce the number of density matrix elements from $\sim N^2$ to $\sim N N_c$ where N_c denotes the number of orbital points of closely lying atoms [36] which communicate coherently upon optical excitation. Typically $N_c \ll N$ results in favorable linear N-scaling of computational effort with size. For example, $N_c \sim 20$ heavy atoms (~ 100 atomic orbitals in semiempirical hamiltonian) in polyenes. This is analogous to similar developments in ground state calculations [37]. We anticipate to achieve $\sim N$ and $\sim N^2$ scaling of memory and total computational time with molecular size, respectively. [3]

The present approach can be extended to compute vibronic structure of electronic transitions by including the dependence of the electronic modes on nuclear coordinates.

Finally, the present analysis was based on the TDHF approximation for the DMRF. The resulting EMS is not equivalent to the original QFM. It simply reproduces its TDHF response. It is possible however to extend this approach and obtain an exact EMS. To that end the QOM should be deformed to yield a bosonized quantum fermion model (BQFM) which will be equivalent to QFM [40–43] (see Fig. 1). The TDHF is then used only to define a convenient set of collective coordinates. These coordinates may then be used to compute the exact DMRF, and we no longer rely on the TDHF. This should result in extending the TDHF equation to include higher-order oscillator variables [22]. The TDHF is then a classical approximation which follows the evolution of a point in phase space. These extensions are semiclassical since they follow the evolution of wavepackets which amounts to including higher moments of the classical variables.

In this paper we have used the single Slater determinants which constitute a set of generalized coherent states [44] for the many-electron problem, to construct the classical limit of the original model. This allowed us to introduce the boson language which has been demonstrated to be useful for developing various approximation schemes. The coherent states form an overcomplete basic set which leads to certain difficulties in using them to describe quantum dynamics. However, they possess the property of the unit operator decomposition [44] which eliminates the difficulties. There are several ways how the coherent states can be used to generate new approximate descriptions of the original many-bodied problem [18,19]. One way is to start with the BQFM which is equivalent to the original QFM, as described in the paper, and derive closed equations of motion for one- and two-boson variables in full analogy with the Frenkel exciton systems [45]. Another way is to use variational dynamical approach by applying Ansätze for the many-body wave function and representing it as a wavepacket in the space of coherent states [18,19]. Finally the coherent states can be used to formulate non-traditional configuration interaction (CI) approaches. Usually the CI schemes take into account certain important configurations which are classified and truncated according to the

---

[3]To calculate the electronic modes of carotenoids (see Section IV) we used the DSMA technique [23] which implements Lanczos-type algorithm and gives $\sim N^2$ and $\sim N^3$ size-scaling of memory and computational time, respectively. We considered molecules of moderate size (~ 40 heavy atoms). These computations are inexpensive and therefore the N-scaling procedure was not implemented.

number of electron-hole pairs, i.e. single CI, double CI, etc. The coherent states allow to introduce new types of configurational spaces. This can be accomplished by defining the configurational space as spanned onto a certain subspace of coherent states. The space of coherent states $\mathbf{M}$ as stated in this paper form a Grassmanian manifold which has a complex analytical structure. We can immerse the complex projective line $\mathbb{CP}^1$ (which is a 1D compact complex manifold) into $\mathbf{M}$ and form a vector subspace in the many-body space of states as generated by the coherent states which belong to $\mathbb{CP}^1$. This should result in a configurational space with the same dimensionality of single CI, which nevertheless contains an arbitrary number of electron-hole pairs.

APPENDIX A: THE CLASSICAL TDHF RESPONSE

To compute the DMRF we recast Eq. (2.20) in the form

$$
i\frac{\partial z_\alpha(t)}{\partial t} = \Omega z_\alpha(t) + \sum_{\beta\gamma} \left(V_{-\alpha-\beta-\gamma} z_\beta^*(t) z_\gamma^*(t) + 2V_{-\alpha-\beta\gamma} z_\beta^*(t) z_\gamma(t) + V_{-\alpha\beta\gamma} z_\beta(t) z_\gamma(t) \right)
$$

$$
- \mathcal{E}(t)\left[\mu_{-\alpha} + \sum_\beta \left(\mu_{-\alpha-\beta} z_\beta^*(t) + \mu_{-\alpha\beta} z_\beta(t) \right) \right] , \tag{A1}
$$

where the summation goes over $\alpha, \beta, \gamma > 0$. This nonlinear equation may be solved by expanding $z(t)$ $(z^*(t))$ in powers of the external field $\mathcal{E}(t)$: $z(t) = z^{(1)}(t) + z^{(2)}(t) + \ldots$. Using the time-domain Green function

$$
G_\alpha(t) = exp(-i\Omega_\alpha t), \tag{A2}
$$

the first order solution of Eq. (A1) is

$$
z_\alpha^{(1)}(t) = i \int_{-\infty}^t d\tau \mathcal{E}(\tau) \mu_{-\alpha} G_\alpha(t - \tau) . \tag{A3}
$$

To second order we obtain

$$
z_\alpha^{(2)}(t) = \int_{-\infty}^t \int_{-\infty}^{\tau_2} d\tau_2 d\tau_1 \mathcal{E}(\tau_2) \mathcal{E}(\tau_1) \sum_\beta \left(\mu_{-\alpha-\beta} \mu_\beta G_\beta^*(\tau_2 - \tau_1) \right.
$$

$$
\left. - \mu_{-\alpha\beta} \mu_{-\beta} G_\beta(\tau_2 - \tau_1) \right) G_\alpha(t - \tau_2) + i \int_{-\infty}^t \int_{-\infty}^t d\tau_2 d\tau_1 \mathcal{E}(\tau_2) \mathcal{E}(\tau_1) \int_{\tau_2}^t d\tau
$$

$$
\times \sum_{\beta\gamma} \left(V_{-\alpha-\beta-\gamma} \mu_\beta \mu_\gamma G_\beta^*(\tau - \tau_2) G_\gamma^*(\tau - \tau_1) - 2V_{-\alpha\beta-\gamma} \mu_{-\beta} \mu_\gamma G_\beta(\tau - \tau_2) G_\gamma^*(\tau - \tau_1) \right.
$$

$$
\left. + V_{-\alpha\beta\gamma} \mu_{-\beta} \mu_{-\gamma} G_\beta(\tau - \tau_2) G_\gamma(\tau - \tau_1) \right) G_\alpha(t - \tau) . \tag{A4}
$$

The time-dependent linear and second-order polarizabilities are given by

$$\mathcal{P}^{(1)} = \sum_{\alpha} \mu_{-\alpha} z_{\alpha}^{*(1)}(t) + \mu_{\alpha} z_{\alpha}^{(1)}(t) , \tag{A5}$$

$$\mathcal{P}^{(2)} = \sum_{\alpha} \mu_{-\alpha} z_{\alpha}^{*(2)}(t) + \mu_{\alpha} z_{\alpha}^{(2)}(t)$$
$$+ \frac{1}{2!} \sum_{\alpha\beta} \left(\mu_{-\alpha-\beta} z_{\alpha}^{*(1)}(t) z_{\beta}^{*(1)}(t) + 2\mu_{\alpha-\beta} z_{\alpha}^{*(1)}(t) z_{\beta}^{(1)}(t) + \mu_{\alpha\beta} z_{\alpha}^{(1)}(t) z_{\beta}^{(1)}(t) \right) , \tag{A6}$$

where $z^{(1)}(t)(z^{*(1)}(t))$ and $z^{(2)}(t)(z^{*(2)}(t))$ are given by Eqs. (A3) and (A4) and their hermitian conjugates. Linear and second-order time-domain response functions are defined by

$$\mathcal{P}^{(1)} = \int d\tau \mathcal{E}(\tau) R^{(1)}(t; \tau) , \tag{A7}$$

$$\mathcal{P}^{(2)} = \int d\tau_2 d\tau_1 \mathcal{E}(\tau_2) \mathcal{E}(\tau_1) R^{(2)}(t; \tau_1, \tau_2) . \tag{A8}$$

Comparing Eqs. (A7) and (A5) (Eqs. (A8) and (A6)) and using Eqs. (A3) and (A4) we obtain for linear and second-order time-domain response function

$$R^{(1)}(t; \tau) = -\sum_{\alpha} \mu_{-\alpha} \mu_{\alpha} (G_{\alpha}(t - \tau) G_{\alpha}^{*}(t - \tau)) , \tag{A9}$$

$$R^{(2)}(t; \tau_1, \tau_2) = i \sum_{\alpha\beta\gamma} \int_{\tau_2}^{t} d\tau \left(V_{-\alpha-\beta-\gamma} \mu_{\alpha} \mu_{\beta} \mu_{\gamma} G_{\alpha}^{*}(\tau - \tau_2) G_{\beta}^{*}(\tau - \tau_1) G_{\gamma}(t - \tau) \right.$$
$$- 2V_{\alpha-\beta-\gamma} \mu_{-\alpha} \mu_{\beta} \mu_{\gamma} G_{\alpha}(\tau - \tau_2) G_{\beta}^{*}(\tau - \tau_1) G_{\gamma}(t - \tau)$$
$$+ V_{\alpha\beta-\gamma} \mu_{-\alpha} \mu_{-\beta} \mu_{\gamma} G_{\alpha}(\tau - \tau_2) G_{\beta}(\tau - \tau_1) G_{\gamma}(t - \tau)) + h.c.$$
$$+ \frac{1}{2!} \sum_{\alpha\beta} \left(2\mu_{-\alpha-\beta} \mu_{\alpha} \mu_{\beta} G_{\alpha}^{*}(\tau_2 - \tau_1) - \mu_{\alpha-\beta} \mu_{-\alpha} \mu_{\beta} G_{\alpha}(\tau_2 - \tau_1) \right) G_{\beta}(t - \tau_2) + h.c.$$
$$- \left(\mu_{-\alpha-\beta} \mu_{\alpha} \mu_{\beta} G_{\alpha}^{*}(t - \tau_1) G_{\beta}^{*}(t - \tau_2) + \mu_{\alpha\beta} \mu_{-\alpha} \mu_{-\beta} G_{\alpha}(t - \tau_1) G_{\beta}(t - \tau_2) \right.$$
$$- 2\mu_{\alpha-\beta} \mu_{-\alpha} \mu_{\beta} G_{\alpha}(t - \tau_1) G_{\beta}^{*}(t - \tau_2)) . \tag{A10}$$

Applying the Fourier transform

$$f(\omega) = \int dt f(t) exp(-i\omega t) ; \qquad f(t) = \frac{1}{2\pi} \int d\omega f(\omega) exp(i\omega t) \tag{A11}$$

to Eqs. (A10) and (A9), we obtain the frequency-dependent linear and second-order polarizabilities

$$P^{(1)}(-\omega_s; \omega) = \int \frac{d\omega}{2\pi} 2\pi \delta(-\omega_s + \omega) \alpha(-\omega_s; \omega) \mathcal{E}(\omega) , \tag{A12}$$

$$P^{(2)}(-\omega_s; \omega_1, \omega_2) = \int \frac{d\omega_1}{2\pi} \frac{d\omega_2}{2\pi} 2\pi \delta(-\omega_s + \omega_1 + \omega_2) \beta(-\omega_s; \omega_1, \omega_2) \mathcal{E}(\omega_1) \mathcal{E}(\omega_2) . \tag{A13}$$

The final expressions for the linear and the second order polarizabilities are:

$$\alpha(\omega) = \sum_{\alpha} \frac{2\mu_{-\alpha} \mu_{\alpha} \Omega_{\alpha}}{\Omega_{\alpha}^2 - \omega^2} , \tag{A14}$$

$$\beta(-\omega_s = \omega_1 + \omega_2; \omega_1, \omega_2) = -\frac{1}{4} \sum_{\alpha\beta\gamma} (V_{\alpha\beta\gamma}\mu_{-\alpha}\mu_{-\beta}\mu_{-\gamma} + h.c.)$$

$$\times \left(\frac{1}{(\Omega_\alpha - \omega_1)(\Omega_\beta - \omega_2)(\Omega_\gamma + \omega_1 + \omega_2)} + \frac{1}{(\Omega_\alpha + \omega_1)(\Omega_\beta + \omega_2)(\Omega_\gamma - \omega_1 - \omega_2)} \right)$$

$$+ (2V_{\alpha-\beta-\gamma}\mu_{-\alpha}\mu_\beta\mu_\gamma + h.c.)$$

$$\times \left(\frac{1}{(\Omega_\alpha + \omega_1)(\Omega_\beta - \omega_2)(\Omega_\gamma + \omega_1 + \omega_2)} + \frac{1}{(\Omega_\alpha - \omega_1)(\Omega_\beta + \omega_2)(\Omega_\gamma + \omega_1 + \omega_2)} \right.$$

$$\left. + \frac{1}{(\Omega_\alpha - \omega_1)(\Omega_\beta + \omega_2)(\Omega_\gamma - \omega_1 - \omega_2)} + \frac{1}{(\Omega_\alpha + \omega_1)(\Omega_\beta - \omega_2)(\Omega_\gamma - \omega_1 - \omega_2)} \right)$$

$$+ (V_{-\alpha\beta\gamma}\mu_\alpha\mu_{-\beta}\mu_{-\gamma} + h.c.)$$

$$\times \left(\frac{1}{(\Omega_\alpha + \omega_1)(\Omega_\beta + \omega_2)(\Omega_\gamma + \omega_1 + \omega_2)} + \frac{1}{(\Omega_\alpha - \omega_1)(\Omega_\beta - \omega_2)(\Omega_\gamma - \omega_1 - \omega_2)} \right)$$

$$+ \frac{1}{4}\frac{1}{2!} \sum_{\alpha\beta} (\mu_{\alpha\beta}\mu_{-\alpha}\mu_{-\beta} + h.c.) \left(\frac{1}{(\Omega_\alpha - \omega_1)(\Omega_\beta + \omega_1 + \omega_2)} + \frac{1}{(\Omega_\alpha - \omega_2)(\Omega_\beta + \omega_1 + \omega_2)} \right.$$

$$+ \frac{1}{(\Omega_\alpha - \omega_1)(\Omega_\beta - \omega_2)} + \frac{1}{(\Omega_\alpha + \omega_1)(\Omega_\beta - \omega_1 - \omega_2)}$$

$$\left. + \frac{1}{(\Omega_\alpha + \omega_2)(\Omega_\beta - \omega_1 - \omega_2)} + \frac{1}{(\Omega_\alpha + \omega_1)(\Omega_\beta + \omega_2)} \right)$$

$$+ 2\mu_{-\alpha\beta}\mu_\alpha\mu_{-\beta} \left(\frac{1}{(\Omega_\alpha + \omega_1)(\Omega_\beta + \omega_1 + \omega_2)} + \frac{1}{(\Omega_\alpha + \omega_2)(\Omega_\beta + \omega_1 + \omega_2)} \right.$$

$$+ \frac{1}{(\Omega_\alpha + \omega_1)(\Omega_\beta - \omega_2)} + \frac{1}{(\Omega_\alpha - \omega_1)(\Omega_\beta - \omega_1 - \omega_2)}$$

$$\left. + \frac{1}{(\Omega_\alpha - \omega_2)(\Omega_\beta - \omega_1 - \omega_2)} + \frac{1}{(\Omega_\alpha + \omega_1)(\Omega_\beta - \omega_2)} \right) \tag{A15}$$

APPENDIX B: SUM-OVER-STATES POLARIZABILITIES OF THE EFFECTIVE MULTILEVEL SYSTEM

In this Appendix we calculate optical polarizabilities for the quantum model QOM using the standard Sum-over-States expressions [1]. The linear and the quadratic polarizabilities are given by

$$\alpha(\omega) = \sum_n \frac{2\omega_{ng}r_{gn}r_{ng}}{\omega_{ng}^2 - \omega^2} \tag{B1}$$

$$\beta(-\omega_s = \omega_1 + \omega_2; \omega_1, \omega_2) = -\frac{1}{4} \sum_{n,n'} r_{gn}r_{nn'}r_{n'g} \left(\frac{1}{(\omega_{n'g} + \omega_1 + \omega_2)(\omega_{ng} + \omega_1)} \right.$$

$$+ \frac{1}{(\omega_{n'g} - \omega_1 - \omega_2)(\omega_{ng} - \omega_1)} + \frac{1}{(\omega_{n'g} + \omega_1 + \omega_2)(\omega_{ng} + \omega_2)} + \frac{1}{(\omega_{n'g} - \omega_1 - \omega_2)(\omega_{ng} - \omega_2)}$$

$$+ \frac{1}{(\omega_{n'g} + \omega_1)(\omega_{ng} + \omega_1 + \omega_2)} + \frac{1}{(\omega_{n'g} - \omega_1)(\omega_{ng} - \omega_1 - \omega_2)} + \frac{1}{(\omega_{n'g} + \omega_2)(\omega_{ng} + \omega_1 + \omega_2)}$$

$$+ \frac{1}{(\omega_{n'g} - \omega_2)(\omega_{ng} - \omega_1 - \omega_2)} + \frac{1}{(\omega_{n'g} - \omega_2)(\omega_{ng} + \omega_1)} + \frac{1}{(\omega_{n'g} + \omega_2)(\omega_{ng} - \omega_1)}$$

$$+ \frac{1}{(\omega_{n'g} - \omega_1)(\omega_{ng} + \omega_2)} + \frac{1}{(\omega_{n'g} + \omega_1)(\omega_{ng} - \omega_2)} \Bigg) , \tag{B2}$$

where the sum runs over all excited states n and n', and g stands for the ground state. $r_{kl} = \langle k|\mathcal{P}|l \rangle$ $(r_{lk} = r_{kl}^*)$ is the transition dipole between k'th and l'th states.

We start with the Hamiltonian (Eq. (3.3)) representing N - quantum oscillators with the electronic polarizability operator $\mathcal{P}(a^+, a)$ (Eq. (3.4). To calculate the transition dipoles we first compute the wavefunctions of our oscillator system to first order in V:

$$\phi^{(0)} = |g\rangle_0 - \frac{1}{3!} \sum_{\alpha\beta\gamma} \frac{V_{-\alpha-\beta-\gamma}}{\Omega_\alpha + \Omega_\beta + \Omega_\gamma} a_\alpha^+ a_\beta^+ a_\gamma^+ |g\rangle_0 \tag{B3a}$$

$$\phi_\alpha^{(1)} = a_\alpha^+ |g\rangle_0 + \frac{1}{3!} \sum_{\beta\gamma} \frac{V_{\alpha-\beta-\gamma}}{\Omega_\alpha - \Omega_\beta - \Omega_\gamma} a_\beta^+ a_\gamma^+ |g\rangle_0 \tag{B3b}$$

$$\phi_{\beta\gamma}^{(2)} = a_\beta^+ a_\gamma^+ |g\rangle_0 - \frac{1}{3!} \sum_\alpha \frac{2V_{-\alpha\beta\gamma}}{\Omega_\alpha - \Omega_\beta - \Omega_\gamma} a_\alpha^+ |g\rangle_0$$

$$+ \frac{1}{3!} \sum_{\delta\zeta} \left(\frac{V_{-\gamma-\delta\zeta} a_\beta^+}{\Omega_\gamma - \Omega_\delta - \Omega_\zeta} + \frac{V_{-\delta-\zeta\beta} a_\gamma^+}{\Omega_\beta - \Omega_\delta - \Omega_\zeta} \right) a_\delta^+ a_m^+ |g\rangle_0 \tag{B3c}$$

where $V_{\alpha\beta\gamma}$ is given by Eq. (2.16c) and $|g\rangle_0$, $a_\alpha^+|g\rangle_0$, $a_\alpha^+ a_\beta^+|g\rangle_0$, and $a_\alpha^+ a_\beta^+ a_\gamma^+|g\rangle_0$ denote the ground, single, double and triple excited states of the uncoupled system respectively.

The transition dipoles among the ground and the first two excited states are given by:

$$\langle \phi^{(0)}|\mathcal{P}|\phi^{(0)} \rangle = 0 , \tag{B4a}$$

$$\langle \phi^{(0)}|\mathcal{P}|\phi_\alpha^{(1)} \rangle = \mu_\alpha , \tag{B4b}$$

$$\langle \phi^{(0)}|\mathcal{P}|\phi_{\alpha\beta}^{(2)} \rangle = \frac{1}{2!}\mu_{\alpha\beta} + 2 \sum_\gamma \left\{ \frac{V_{\alpha\beta-\gamma}\mu_\gamma}{\Omega_\alpha + \Omega_\beta - \Omega_\gamma} - \frac{V_{\alpha\beta\gamma}\mu_{-\gamma}}{\Omega_\alpha + \Omega_\beta + \Omega_\gamma} \right\} , \tag{B4c}$$

$$\langle \phi_\alpha^{(1)}|\mathcal{P}|\phi_\beta^{(1)} \rangle = \mu_{-\alpha\beta} + \sum_\gamma \left\{ \frac{V_{\alpha\beta-\gamma}\mu_{-\gamma}}{\Omega_\alpha - \Omega_\beta - \Omega_\gamma} + \frac{V_{-\alpha-\beta\gamma}\mu_\gamma}{-\Omega_\alpha + \Omega_\beta - \Omega_\gamma} \right\} , \tag{B4d}$$

$$\langle \phi_\alpha^{(1)}|\mathcal{P}|\phi_{\alpha\beta}^{(2)} \rangle = \mu_\beta . \tag{B4e}$$

Substituting these transitions dipoles in Eqs. (B1) and (B2) we obtain expressions for the linear and the second-order polarizabilities which coincide with Eqs. (A14) and (A15). This proves the equivalence of the linear and the second-order polarizabilities of the QOM calculated in the classical limit and using the Sum-over-States expression.

APPENDIX C: NONLINEAR RESPONSE OF SYSTEMS WITH COORDINATE-DEPENDENT ANHARMONICITIES

When the anharmonicities in Eqs. (3.3) and (3.4) only depend on coordinates $q_\alpha = (a_\alpha^+ + a_\alpha)q_{0\alpha}/\sqrt{2}$ (and not on the momenta $p_\alpha = (a_\alpha^+ - a_\alpha)p_{0\alpha}/\sqrt{2}$) the DMRF are simplified considerably. In this case we have

$$V_{\alpha\beta\gamma} = V_{-\alpha-\beta-\gamma} = V_{-\alpha\beta\gamma} = V_{-\alpha-\beta\gamma} \equiv V_{\alpha\beta\gamma}^q \frac{q_{0\alpha}q_{0\beta}q_{0\gamma}}{\left(\sqrt{2}\right)^3} , \tag{C1}$$

$$\mu_{-\alpha-\beta} = \mu_{\alpha\beta} = \mu_{-\alpha\beta} \equiv \mu_{\alpha\beta}^q \frac{q_{0\alpha}q_{0\beta}}{\left(\sqrt{2}\right)^2} , \tag{C2}$$

$$\mu_\alpha = \mu_\alpha \equiv \mu_\alpha^q \frac{q_{0\alpha}}{\sqrt{2}} . \tag{C3}$$

The time-domain response (Eq. (A10)) then becomes

$$R(t;\tau_1,\tau_2) = -\int_{\tau_2}^t d\tau \sum_{\alpha\beta\gamma} V_{\alpha\beta\gamma}^q \mu_\alpha^q \mu_\beta^q \mu_\gamma^q \frac{(q_{0\alpha}q_{0\beta}q_{0\gamma})^2}{8} C_\alpha(\tau-\tau_2)C_\beta(\tau-\tau_1)C_\gamma(t-\tau)$$

$$+ \sum_{\alpha\beta} \mu_{\alpha\beta}^q \mu_\alpha^q \mu_\beta^q \frac{(q_{0\alpha}q_{0\beta})^2}{4} \left(2C_\alpha(\tau_2-\tau_1)C_\beta(t-\tau_2) + C_\alpha(t-\tau_1)C_\beta(t-\tau_2)\right) , \tag{C4}$$

where

$$C_\alpha(t) = i(G_\alpha(t) - G_\alpha^*(t)) = 2\sin(\Omega_\alpha t) , \tag{C5}$$

is the classical linear response of a harmonic oscillator.

Similarly Eq. (A15) reduces to

$$\beta(-\omega_s = \omega_1 + \omega_2; \omega_1, \omega_2) = -\sum_{\alpha\beta\gamma} \frac{V_{\alpha\beta\gamma}^q \mu_\alpha^q \mu_\beta^q \mu_\gamma^q}{M_\alpha M_\beta M_\gamma} \frac{1}{(\Omega_\alpha^2 - \omega_1^2)(\Omega_\beta^2 - \omega_2^2)(\Omega_\gamma^2 - (\omega_1+\omega_2)^2)}$$

$$+ \sum_{\alpha\beta} \frac{\mu_{\alpha\beta}^q \mu_\alpha^q \mu_\beta^q}{M_\alpha M_\beta} \left(\frac{1}{(\Omega_\alpha^2 - \omega_1^2)(\Omega_\beta^2 - (\omega_1+\omega_2)^2)} \right.$$

$$\left. + \frac{1}{(\Omega_\alpha^2 - \omega_2^2)(\Omega_\beta^2 - (\omega_1+\omega_2)^2)} + \frac{1}{(\Omega_\alpha^2 - \omega_1^2)(\Omega_\beta^2 - \omega_2^2)} \right) . \tag{C6}$$

[1] J.F. Ward, *Rev. Mod. Phys.*, **37**, 1, (1965); B.J. Orr, J.F. Ward, *Mol. Phys.*, **20**, 513, (1971).

[2] *Nonlinear Optical Properties of Organic Molecules and Crystals*, Vol. **1, 2**, J. Zyss and D.S. Chemla, Eds. (Academic Press, Orlando, 1987).

[3] D.R. Kanis, M.A. Ratner, and T.J. Marks, *Chem. Rev.*, **94**, 195 (1994).

[4] J.L. Brédas, C. Adant, P. Tackyx, A. Persoons, and B.M. Pierce, *Chem. Rev.* **94**, 243 (1994).

[5] S.A. Kicharski, R.J. Bartlett, *J. Chem Phys.* **97**, 4282 (1992); *J. Chem Phys.* **95**, 8227 (1991); H. Sekino and R.J. Bartlett, *J. Chem. Phys.* 94, 3665, (1991).

[6] J. A. Pople, P. M. W. Gill, and B. J. Johnson, *Chem. Phys. Lett.* **199**, 557 (1992).

[7] A. D. Becke, *Phys. Rev. A* **38**, 3098 (1988).

[8] E. K. U. Gross, J. F. Dobson and M. Petersilka, in *Density Functional Theory*, edited by R. F. Nalewajski, volume 181, pages 1-81, Springer, Berlin, 1996.

[9] R. G. Parr and W. Yang *Density-functional theory of atoms and molecules*, (Oxford University Press, Oxford, 1994).

[10] M. E. Casida, in *Recent Advances in Density-Functional Methods*, Part I, edited by D.A. Chong, volume 3, pages 155–192, World Scientific, Singapore, 1995.

[11] C. Jamorski, M.E. Casida, and D.R. Salahub, *J. Chem. Phys.* **104**, 5134 (1996).

[12] P. Hohenberg and W. Kohn, *Phys. Rev.* **136**, B864 (1964).

[13] W. Kohn and L. J. Sham *Phys. Rev.* **140**, A1133 (1965).

[14] A. Szabo and N.S. Ostlund, *Modern Quantum Chemistry: Introduction to Advanced Electronic Structure Theory* (McGraw-Hill, New York, 1989).

[15] R. McWeeny and B.T. Sutcliffe, *Methods of Molecular Quantum Mechanics* (Academic Press, New York, 1976); E.R. Davidson, *Reduced Density Matrices in Quantum Chemistry* (Academic Press: New York, 1976).

[16] P.O. Lowdin, *Phys. Rev.* **97**, 1474, (1955); *Adv. in Phys.* **5**, 1, (1956).

[17] R.S. Milliken, *J. Chem. Phys.*, **23**, 1833, 1841, 2338, 2343, (1955).

[18] P.Ring and P.Schuck, *The Nuclear Many-Body Problem* (Springer-Verlag, New York, 1980).

[19] J.-P. Blaizot and G. Ripka, *Quantum Theory of Finite Systems* (The MIT Press, Cambridge, Massachusetts, London, England, 1986).

[20] H. Sekino and R. J. Bartlett, *J. Chem. Phys.* **98**, 3022 (1993).

[21] V. Chernyak, S. Mukamel, *J.Chem.Phys.* **104**, 444 (1996).

[22] V. Chernyak and S. Mukamel, *J.Chem.Phys.* **108**, 5812 (1998).

[23] S. Tretiak, V. Chernyak and S. Mukamel, *JACS* **119**, 11408 (1996).

[24] L. D. Landau and E. M. Lifshitz, *Mechanics* 3rd ed. (Oxford, New York : Pergamon Press, 1976).

[25] Vincent Ricci, *Large Enhancement of Third Order Susceptibility*, MS Thesis, Dept. of Electrical Engineering, University of Central Florida (1995).

[26] S. Mukamel, S. Tretiak, T. Wagersreiter, and V. Chernyak, *Science*, **277**, 781 (1997).

[27] S. Tretiak, V. Chernyak and S. Mukamel, *Chem.Phys.Lett.* **259**, 55 (1996); S. Tretiak, V. Chernyak and S. Mukamel, *J. Chem. Phys.*, **105**, 8914 (1996).

[28] S. Tretiak, V. Chernyak, and S. Mukamel, *J. Phys. Chem. B*, **102**, 3310-3315 (1998).

[29] S. Tretiak, V. Chernyak, and S. Mukamel, *Chem. Phys. Lett.*, **287**, 75-82 (1998), S. Tretiak, V. Chernyak, and S. Mukamel (unpublished).

[30] J. Ridley and M.C. Zerner, *Theor. Chim. Acta*, **32**, 111 (1973).

[31] M.C. Zerner, G.H. Loew, R.F. Kirchner, and U. T. Mueller - Westerhoff, *J. Am. Chem. Soc.*, **102**, 589 (1980).

[32] J.A. Pople and G.A. Segal *J. Chem. Phys.*, **43**, S136 (1965); J.A. Pople D.L. Beveridge, and P. Dobosh, *J. Chem. Phys.*, **47**, 2026 (1967).

[33] G. C. Bazan, W. J. Oldham, Jr., R. J. Lachicotte, S. Tretiak, V. Chernyak, and S. Mukamel, *J. Am. Chem. Soc.*, **120**, 9188-9204 (1998).

[34] J. Baker and M. Zerner, *Chem. Phys. Lett.*, **175**, 192, (1990).

[35] S. Tretiak, V. Chernyak, and S. Mukamel (unpublished).

[36] O. Dubovsky, and S. Mukamel, *J. Chem. Phys.*, **95**, 7828 (1991).

[37] E. Schwegler, M. Challacombe, M. Head-Gordon, *J. Chem. Phys.*, **106**, 9708 (1997).

[38] Y. Yamaguchi, J. Cow, H. F. Schaefer, and J.S. Binkley, *J. Chem. Phys.*, **84**, 2262 (1986); B.G. Johnson and M.J. Frisch, *J. Chem. Phys.*, **100**, 7429 (1994)

[39] H.B. Schlegel, J.S. Binkley, and J.A. Pople, *J. Chem. Phys.*, **80**, 1976 (1984).

[40] F. J. Dyson, *Phys. Rev.*, **102**, 1217 (1956).

[41] V. M. Agranovich and B. S. Toshich, *Zh. Éksp. Teor. Fiz.*, **53**, 281 (1967) [Sov. Phys. JETP **26**, 188 (1968).

[42] T. Holstein and H. Primakoff, *Phys. Rev. B*, **58**, 1098 (1940).

[43] V. Chernyak, *Phys. Lett. A*, **163**, 117 (1992).

[44] A. Perelomov, *Generalized Coherent States and their applications*, (Springer, Berlin, 1986).

[45] S.Mukamel, *Principles of Nonlinear Optical Spectroscopy* (Oxford, New York, 1995).